韓國鑛物學會誌 第 9 卷 第 2 號(1996)
J. Miner. Soc. Korea, 9, 55-63(1996)

FTIR and Mössbauer Spectroscopic Studies on the Hydrothermal Epidote from the Bobae Clay Deposit, Pusan, Korea

보배광산에서 산출하는 열수변질 기원 녹염석의 분광학적 특성 : 적외선 및 뫼스바우어 연구

Chang Oh Choo (추창오) · Soo Jin Kim (김수진)

Department of Geological Sciences, Seoul National University, Seoul 151-742, Korea
(서울대학교 지질과학과)

ABSTRACT : Epidote occurs as veinlets in the propylitic alteration zone of the Bobae clay deposit, Pusan, Korea. Its cell parameters apparently decrease with the contents of Al, Fe, and Ca. Fourier transform infrared (FTIR) spectra show one hydroxyl environment related to Al_{M2} at 3357-3358 cm^{-1}. In the mid-infrared region, the peaks at 950 and 1030 cm^{-1} become sharper with increasing Al shifting to higher energy region. The peak at 885 cm^{-1} shifts slightly to a lower energy region with a decreasing intensity as the Fe content increases. In the far-IR region, epidote exhibits absorption bands at 120 and 140 cm^{-1}, which are related to the Ca-O bonds in A-sites.

Mössbauer spectra of epidote show that the isomer shifts of Fe^{3+} range from 0.36-0.37 at the M3 site and from 0.35-0.44 at M1 site. Fe^{2+} shows the isomer shift ranging from 1.11 to 1.13. Quadrupole splitting is 2.04 for $Fe^{3+}{}_{M3}$, 0.52-0.70 for $Fe^{3+}{}_{M1}$, and 2.61-2.70 for $Fe^{2+}{}_{M3}$. Calculation shows $Fe^{3+}{}_{M3}$ 86-90.7 %, $Fe^{3+}{}_{M1}$ 2.5-3.5 %, and $Fe^{2+}{}_{M3}$ 5.8-11.4 % of total iron, showing preferential distribution of Fe^{3+} in the M3 site. The $Fe^{3+}{}_{M3}$ content is between 0.486 and 0.513 per formula unit. In the Fe-rich epidote, less Fe^{3+} and more Fe^{2+} are accommodated in the M1 and M3 sites. Hence, the overall disorder increases as total Fe content increases. The ordering parameter of the Bobae epidote is 0.93-0.95, suggesting a disequilibrium state below 200 ℃. The constant temperature over a long period may be essential for the transition from disordered state to equilibrium state, despite the possible variation in flux and composition of the hydrothermal fluid.

요약 : 맥상의 녹염석이 부산 강서구 보배 광산의 프로피리틱 변질대에서 나타난다. 녹염석은 Al, Fe, Ca함량 높을 수록 단위포 상수의 값은 다소 작다. 푸리에변환 적외선분광분석 결과 3357~3358 cm^{-1}에서 한개의 (OH)기의 흡수선이 관찰되는데 이는 M2 자리의 Al과 관련되어 있다. 950, 1030 cm^{-1}에서의 흡수선은 Al의 함량이 증가할수록 강도가 증가하며 885 cm^{-1}에서의 흡수선은 Fe가 증가할수록 저에너지 영역으로 변위한다. 원적외선 영역에서는 120, 140 cm^{-1}에서 두개의 흡수선을 보이는데 이들은 A자리의 Ca와 관련되는 것으로서 비교적 약한 결합을 이룬다.

뫼스바우어 분광분석 결과 isomer shift는 $Fe^{3+}{}_{M3}$가 0.36-0.37, $Fe^{3+}{}_{M1}$는 0.35-0.44, $Fe^{2+}{}_{M1}$는 1.11-1.13 범위를 보인다. 또한 Quadrupole splitting은 $Fe^{3+}{}_{M3}$가 2.04, $Fe^{3+}{}_{M1}$, 0.52-0.70, $Fe^{2+}{}_{M3}$는 2.61-2.70이다. 이를 함량비로 계산하면 $Fe^{3+}{}_{M3}$ 86-90.7 %, $Fe^{3+}{}_{M1}$ 2.5-3.5%, and $Fe^{2+}{}_{M3}$ 5.8-11.4%가 되는데 주로 M3 자리에 Fe^{3+}가 집중적으로 분포한다. Fe함량이 높을수록 Fe^{3+}는 M1, M3 자리에 덜 들어가는 반면에, Fe^{2+}는 보다 많이 들어간다. Ordering parameter는 0.93-0.95 정도로

200 ℃ 이하에서 결정화되었음을 시사한다.

보배광상의 변질작용이 비교적 오래동안 지속되었음을 볼 때, 비록 열수용액의 조성이나 유체의 변화가 어느 정도 있음을 감안하더라도 이같은 변질작용의 환경이 녹염석의 무질서도-평형상태에 영향을 미쳤을 것으로 여겨진다.

INTRODUCTION

Epidote is commonly found as one of the alteration products of hydrothermal fluid-rock interaction. Hence it occurs widely in the alteration zones of many hydrothermal ore deposits or in geothermal areas (Keith et al., 1968; Bird and Helgeson, 1981; Bird et al., 1984; Shikazono, 1984; Caruso et al., 1988, Kim et al., 1994). Extensive hydrothermal alteration has been reported from the Late Cretaceous volcanic rocks in the southeastern part of the Korean peninsula (Kim et al., 1991, 1994). Several clay deposits were formed by the hydrothermal alteration of volcanic rocks in the Pusan-Kimhae area. These deposits produce illite, pyrophyllite, and kaolin-rich clays. Epidote is often found in the propylitic alteration zone of clay deposits in this area. It generally shows great diversity in chemical composition and zoning. Most epidotes show fluctuation in chemical composition depending on the bulk composition of host rocks, temperature, pressure, oxygen fugacity, CO_2, and pH of the solution (Raith, 1976; Grapes and Watanabe, 1984; Shikazono, 1984; Bird et al., 1988; Caruso et al., 1988; Anarson and Bird, 1992). Moreover, their chemistry is not simply controlled by a single factor. For instance, Patrier et al. (1991) observed no correlation in the Fe contents of host rock and epidote.

Spectroscopic study is useful for the characterization of structures, Fe assignments, and bonding states of constituent atoms in epidote. Mössbauer spectra of epidotes formed at various P-T environments have been reported by previous workers (Bancroft et al., 1967; Dollase, 1973; Paesano et al., 1983). Their works mainly focused on the Fe site assignments and ordering state in epidotes. Mössbauer studies on epidotes from a single geothermal area were carried out by Bird et al. (1988) and Patrier et al. (1991). They used zoned epidote from veins exhibiting some ranges in chemistry. Therefore, it is difficult to state that their data represent the optimum data concerning oxidation state or site assignment of Fe at a constant pistacite component (X_{Ps}=Fe/Fe+Al) with certainty. Infrared spectroscopy was frequently utilized in assigning the states of atomic bondings in epidote and it was generally performed in the mid-infrared region by a few workers (Langer and Raith, 1974; Langer and Lattard, 1980). But none of spectroscopic data in the far-infrared region has been reported so far.

The purpose of the present study is to characterize the spectroscopic properties of epidotes of homogeneous composition using Fourier transform infrared (FTIR) spectroscopy and Mössbauer spectroscopy. Especially FTIR data were obtained from mid- to far-IR regions.

OCCURRENCE OF EPIDOTE

The geology of the Pusan-Kimhae area in the southeastern part of Korean peninsula is composed of sedimentary rocks of the Hayang Group and the volcanic rocks of the Yucheon Group of Late Cretaceous, and the Bulgugsa intrusive rocks of Late Cretaceous to Early Tertiary. The Yucheon Group consists of volcanic and subordinate sedimentary rocks. The Bobae deposit is one of the major clay deposits which were formed in the volcanic rocks in the Pusan-Kimhae area. The geology around the deposit is composed of the Late Cretaceous rhyodacitic tuff, granodiorite, and quartz porphyry. The Bobae deposit might be hydrothermal alteration product related

to the intrusion of granodiorite (Kim et al., 1991; Moon, 1994). Rhyodacitic tuff is widely distributed in the northern part of the Bobae deposit, while granodiorite occurs as intrusion into the rhyodacitic tuff in the southern part of the deposit. The tuff is generally grey and/or greenish grey but rarely greyish white, probably due to leaching of mafic minerals during hydrothermal alteration. It also shows welding structure of flattened glassy clasts. Most crystal fragments are quartz, K-feldspar and plagioclase, whereas the matrix is composed of glass and fine-grained plagioclase. The resorption embayments are observed in some quartz and feldspar grains. Alteration of the host rocks is characterized by the sericitic and propylitic alteration zones (Kim et al., 1991).

Epidote occurs as replacement of feldspar or veinlets in the propylitic zone of the Bobae deposit. Epidote-bearing paragenesis is observed over the large area as far as 2-3 km from the deposit. It is closely associated with plagioclase, chlorite, calcite, pyrite, and quartz. Epidote crystal replacing plagioclase commonly shows anhedral to subhedral forms and exhibits homogeneous compositions. But the strong zonal structures are also observed in places. Epidotization is generally detected at the margin or along fractures of plagioclase. Thin quartz veins cut epidote-rich veins. Most epidotes in veinlets are usually equigranular and show very weak or no zoning. The size of epidote varies from place to place, ranging from 50 to 200 μm in length. Since epidote forms in the late stage of hydrothermal alteration and occurs in the propylitic alteration zone, its formation temperature would not be high.

EXPERIMENTAL METHODS

Identification and structural characterization of epidotes were made using a X-ray diffractometer. A Rigaku RAD3-C, automated X-ray diffractometer equipped with a Cu target and Kα radiation, was operated at 40 kV/30 mA and 0.5°-0.15 mm-1.0° slits. For structural analysis of pure monominerals, X-ray diffraction data were recorded on the step scan mode. The intensity data were counted for 3 seconds per each 0.02° step from 5 to 70° 2θ.

Chemical analysis of epidotes was performed using a Cameca SX50 electron microprobe fitted with automated wavelength-dispersive spectrometer operated at 1 μm beam diameter, 20 kV accelerating voltage and 15 nA beam current, with 20-seconds counts per element. Both Na and K were counted first so as to avoid alkali loss during the analyses. Quantitative analyses were performed using a ZAF correction.

Infrared spectra were obtained using a Bomem DA-8 Fourier transform infrared (FTIR) spectrometer. The FTIR spectrometer incorporates a KBr beamsplitter and a mercury-cadmium-telluride detector (MCT) cooled by liquid-nitrogen for the mid-IR range. Liquid-helium-cooled Bolometer was adapted for the far-IR experiment. All the samples were prepared by the pellet technique. FTIR spectra in the mid-IR region were recorded in the frequency range 400-4000 cm^{-1}, with resolution of 1 cm^{-1}. In the present study, teflon is first used as a matrix material for the far-infrared experiment because it does not give any spectra overlapped with those of clay minerals. Far-infrared absorption spectra were recorded in the 50-200 cm^{-1} region, with the resolution of 0.2 cm^{-1}. During the experiments the FT spectrometer was operated under the vacuum condition and purged with dry nitrogen in order to remove atmospheric water vapor.

For Mössbauer spectroscopy all spectra were recorded with a source of ^{57}Co in Rh matrix with an activity of 10 mCi. The transmitted radiation was recorded at S600 Mössbauer spectrometer using 1024 channels of a multichannel analyzer. The purified samples were ground with acetone in order to prevent Fe ions from oxidizing. Velocity of each spectrum was calibrated relative to metallic Fe. Deconvolutions of spectra obtained

were evaluated by a least squares fitting program, assuming Lorentzian line shapes.

RESULTS AND DISCUSSIONS

Epidote Chemistry

Chemistry of vein epidotes were analyzed using electron microprobe. Fe was assumed to be ferric. Chemical analysis shows SiO_2 37.04-37.92, Al_2O_3 24.28-25.40, Fe_2O_3 10.17-11.28, and CaO 23.49-24.33 wt%. The mole % of pistacite component (that is, X_{PS}=Fe/Fe+Al) in epidotes is 20.4-22.7. The standard deviations of the pistacite component are small in vein epidotes, indicating relatively homogeneous compositions. It suggests that variation in temperature, flux, and composition of hydrothermal fluids was not significant during the formation of vein epidotes because the Fe/Fe+Al ratio varies with these factors (e. g. Bird et al., 1988; Patrier et al., 1991). Structural formulae of epidotes are $Ca_{2.01}(Al_{2.3}Fe_{0.68}Mn_{0.03})(Si_{2.98}Al_{0.02})O_{12}(OH)$ for sample BJ1-1 and $Ca_{2.0}(Al_{2.28}Ti_{0.01}Fe_{0.64}Mg_{0.02}Mn_{0.02})(Si_{3.01})O_{12}(OH)$ for sample B7-25, respectively.

Vein epidotes do not always exhibit homogeneous composition. For instance, Bird et al. (1988) reported that vein epidotes from the active geothermal system exhibit a wide range in Fe^{3+}-Al exchange.

Unit Cell Parameters of Epidote

The unit cell parameters of epidote calculated from the powder XRD data are a=8.825 Å, b=5.598 Å, c=10.118 Å, and β=115.272° for sample BJ1-1 and a=8.871 Å, b=5.614 Å, c=10.141 Å, and β=115.515° for sample B7-25. There have been several studies of the variation of cell parameters with respect to chemistry in epidotes. Seki (1959) shows qualitatively that a, b, c, and V all increase with $Fe^{3+}/(Fe^{3+}+Al)$ ratio. Myer (1965) demonstrates approximately linear relationships for each of these parameters for epidotes with low Mn content. However, such structural properties are not found in the vein epidotes from the Bobae mine. Rather, epidotes of high Al, Fe, and Ca contents show slightly smaller cell parameters. The variations in cell parameters are insignificant in epidotes showing apparent correlation of unit cell parameters with the iron content.

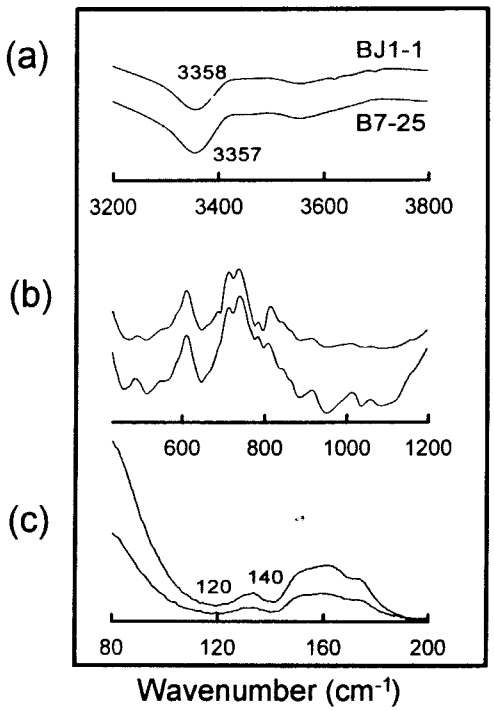

Fig. 1. Infrared spectra of epidotes in the mid- and far-IR region.

FTIR Spectroscopy

Mid-IR Region. One broad OH stretching vibration band is observed at 3357-3358 cm^{-1} region (Fig. 1). It is attributed to hydroxyl bound to octahedral Al. Langer and Raith (1974) show that positions of OH vibration in clinozoisite shift to higher energy frequency with increasing Fe^{3+} content. According to Deer et al. (1986), the band positions and shapes in the infrared ranges can be used to distinguish orthorhombic from monoclin-

ic species. They show an additional band at 2160 cm^{-1} in orthorhombic. Epidotes from the Bobae mine do not show such a band, indicating that these are monoclinic.

The Si-O stretching vibration occurs in the region of 800-1000 cm^{-1}, the SiOSi symmetrical stretching band in the region of 600-700 cm^{-1}, and the Si-O bending mode in the region of 650-475 cm^{-1} (Vedder, 1964; Farmer, 1974). The peaks at 950 and 1030 cm^{-1} become sharper and shift to higher wavenumbers with increasing Al. The substitution of Fe^{3+} for Al in the octahedral sites causes the increase of attractive force of octahedral sites, giving rise to shifting of the band toward the low frequency. The peak at 885 cm^{-1} shifts slightly to a lower wavelength region and decreases in intensity as the Fe content increases. Epidote having higher Fe shows sharper bands at 800 cm^{-1}. The peak at 520-525 cm^{-1} becomes sharper and shifts toward higher energy regions with increasing Ca content.

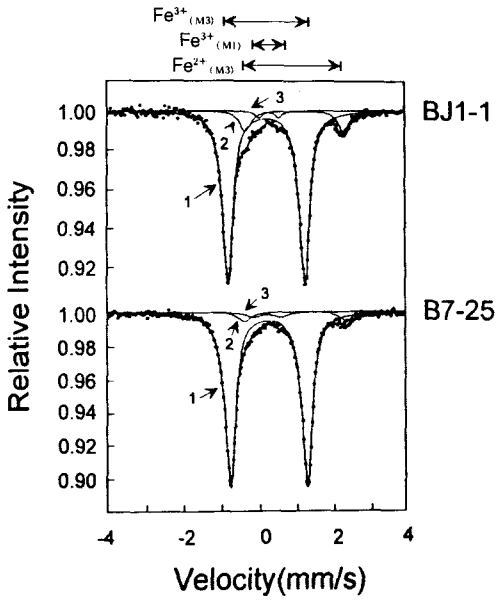

Fig. 2. Mössbauer spectra of epidotes. Samples BJ1-1 (upper) and B7-25 (bottom) show slightly different pattern. Lines 1=Fe^{3+}_{M3}, 2=Fe^{3+}_{M1}, and 3=Fe^{2+}, respectively.

Far-IR Region. In the far-infrared region, spectroscopic data of epidote have not been yet reported in the literature. In the far-infrared range, two bands are observed at 120 cm^{-1} and 140-141 cm^{-1}. The vibrations in this range are related to interlayer M-O stretching modes or interlayer ion translations (Ishii et al. 1967). In the epidote structure, Ca enters into the A-sites which are nine- to ten-coordination slightly different from the interlayer sites in muscovite. Therefore, absorption bands related to the Ca-O bond in the sites appear slightly higher frequencies. In the far-IR and OH stretching ranges, the variation in peak positions due to the different Fe and Ca contents is not significant. Epidote containing higher Fe and Ca contents shows bands of relatively stronger intensity.

Mössbauer Spectroscopy

Mössbauer spectra of epidotes from various conditions have been reported by previous workers (Bancroft et al., 1967; Dollase, 1973). Their works are mainly focused on the Fe site assignments and ordering state in epidotes. Mössbauer studies on epidotes from a single geological setting were carried out by Bird et al. (1988) and Patrier et al. (1991). They used zoned crystals mostly from veins which show still distinct zoning in chemical composition. The Fe occupancy determined might be the average of zoned epidotes.

The same epidote samples used for the FTIR experiment were studied using Mössbauer spectroscopy. Mössbauer spectra of epidote are shown in Fig. 2. The large outer doublets represent Fe^{3+}_{M3} and smaller inner doublets are Fe^{3+}_{M1}, respectively. For high-spin compound, the chemical shift for Fe^{2+} is larger than that for Fe^{3+} compared with the same ligands. The isomer shift of Fe^{2+} is always greater than that of Fe^{3+} in high spin situations. As the occupation of the d orbitals with high coordination number increases, the chemical

Table 1. Characters of Mössbauer spectra of epidotes from the Bobae mine.

sample	line	assign-ment	IS (mm/s)	QS (mm/s)	area (%)
BJ1-1	1	Fe^{3+}_{M3}	0.36	2.04	86.0
	2	Fe^{2+}_{M3}	1.13	2.61	11.4
	3	Fe^{3+}_{M1}	0.44	0.52	2.5
B7-25	1	Fe^{3+}_{M3}	0.37	2.04	90.7
	2	Fe^{2+}_{M3}	1.11	2.70	5.8
	3	Fe^{3+}_{M1}	0.35	0.70	3.5

shift increases. With increasing oxidation state the isomer shift decreases because of an increase in the electron density within the nuclei. The isomer shift of Fe^{3+} ranges from 0.36 to 0.37 at the M3 site and ranges from 0.35 to 0.44 at M1 site (Table 1). Fe^{2+} shows the isomer shift ranging from 1.11 to 1.13. According to Maddock (1985), the isomer shift for octahedral Fe^{2+} ranges 1.1–1.43, whereas the shift for Fe^{3+} in the same coordination ranges from 0.60 to 0.78. The present study shows that isomer shift of Fe^{2+} is similar to his data but Fe^{3+} values are much lower relative to his data. The quadrupole splitting is 2.04 for Fe^{3+}_{M3}, 0.52–0.70 for Fe^{3+}_{M1}, and 2.61–2.70 for Fe^{2+}_{M3}. The spectral data show Fe^{3+}_{M3} 86.0–90.7 %, Fe^{3+}_{M1} 2.5–3.5 %, and Fe^{2+}_{M3} 5.8–11.4 %. In comparison with data obtained from the electron microprobe analysis, epidote of higher total Fe content also has higher Fe^{2+} content. Redhammer et al. (1993) have shown that with increasing Fe^{3+} content on octahedral sites in annites the quadrupole splitting of Fe^{3+} increases, whereas the isomer shift of Fe^{3+} decreases. However, the epidotes from the Bobae mine show that with increasing Fe^{3+}_{M3} content the quadrupole splitting slightly decreases, whereas the isomer shift is nearly constant on the Fe^{3+}_{M3} site. There is no evidence of the presence of tetrahedral iron in epidotes from the Bobae mine.

Nonequilibrium ordering states are typical of epidote minerals in various geological environments (Bird et al., 1988; Franz and Selverstone, 1992). The exchange of Fe^{3+} and Al in epidote is complicated by intracrystalline substitutional order/disorder in the M1 and M3 octahedral sites. If a completely ordered epidote contains Fe^{3+} ions only in the M3 site, the octahedral disordering can be written as $Fe^{3+}_{M3} + Al^{3+}_{M1} = Fe^{3+}_{M1} + Al^{3+}_{M3}$. As $X_{Fe3+,M1}$ increases, disordering increases. M2 site accommodates only Al, whereas M3 site contains a larger fraction of Fe^{3+} compared to the smaller M1 site. As the content of Fe^{2+} increases, disordering also increases because octahedral Fe^{2+} has larger ionic radius than Fe^{3+}. Since total Fe content is low in epidote from the Bobae mine, the Fe^{3+} ion assigned to the M3 site is also low; $0.486 < X_{Fe3+,M3} < 0.513$ per formula unit. Langer and Raith (1974) proposed that in clinozoisite-epidote series with Fe^{3+} contents up to 0.8 Fe^{3+} per formula, the M1 and M2 octahedra are nearly free of Fe^{3+}. However, although total Fe content in epidote from the Bobae mine is relatively low per formula unit, the Fe^{3+} content in the M1 site is 2.5–3.5 % of total Fe. Therefore, the Fe^{3+} content attributed to M1 site does not appear to strictly depend on the total Fe content. In the more Fe-rich epidote, less Fe^{3+} and more Fe^{2+} are accommodated in the M1 and M3 sites. As a consequence, overall disordering increases as total Fe content increases, although further data on many epidote samples should be needed to ascertain this hypothesis.

Disordering in epidote is also largely controlled by temperature. With increasing temperature, the Fe^{3+} content of the M1 site decreases in epidotes from the Salton Sea geothermal system (Bird et al., 1988). The ordering parameter ($0 = 1 - 2X_{Fe3+,M1}$) by Bird and Helgeson (1980) are 0.99 at 25 ℃, 0.90 at 200 ℃, 0.85 at 300 ℃, and 0.74 at 600 ℃, respectively. On the basis of Fe^{3+}_{M1} occupancy, the ordering parameters in epidotes of the Bobae mine are calculated to 0.93–0.95, which implies disequilibrium state of order/disorder below 200 ℃. Because most epidotes reported in the literature occur in active geothermal systems, pegma-

tites, skarns, high grade metamorphic rocks, or plutonic rocks, their formation temperature is relatively high. Therefore, an average ordering parameter is perhaps lower than ours. Dollase (1973) reports that the ordering parameter is about 0.85 for most natural epidotes. Epidotes crystallized at temperatures lower than 300 ℃ show an increase of the nonequilibrium ordering state (Patrier et al., 1991). Considering the ordering parameter, the epidote from the Bobae mine was probably formed at lower temperature than epidotes reported by Dollase (1973).

According to the isotope data on the Bobae deposit by Moon (1994), the character of initial hydrothermal fluids derived from residual magma changed due to introduction of meteoric water during the later stage and hydrothermal alteration persisted over at least 15 m. y. The constant temperature over a long period might be essential for the transition from disordered state to equilibrium state, despite the possible variation in flux and composition of the hydrothermal fluid.

Epidotes studied previously by Mössbauer spectroscopy commonly show distinct zoning in chemical composition though most samples were collected from veins or vugs (e. g. Bird et al., 1988; Patrier et al., 1991). For example, the X_{PS} (=Fe/(Fe+Al) ranges from 0.23-0.41, with the average variation of X_{PS}=0.1 within a single sample (see Bird et al., 1988). The most disordered epidotes also exhibit the widest range in X_{PS}. Their observations might be due to the effect of ordering on chemical zoning in epidotes. Hence its effect should be taken into account in Mössbauer result.

CONCLUSIONS

Vein epidotes occurring in the propylitic alteration zone of the Bobae clay deposit show little or very weak zoning. Epidote of higher Al, Fe, and Ca contents shows slightly smaller cell parameters. FTIR spectra show that the substitution of Fe for Al causes peak positions to shift to a lower energy region and a decrease in the absorption intensity. In the far-IR region, epidotes exhibit two absorption bands, which are related to the Ca-O bonds in A-sites.

These bands apparently show no trend in peak positions with respect to the Fe and Al contents possibly due to their weak bondings, as is the case for the interlayer sites of clay minerals.

Mössbauer spectra of epidote show a preferential distribution of Fe^{3+} in the M3 sites. In Fe-rich epidote, less Fe^{3+} and more Fe^{2+} are accommodated in the M3 and M1 sites. As a consequence, overall disordering increases as total Fe content increases. The ordering parameters of the Bobae epidote imply a disequilibrium state below 200 ℃. The constant temperature over a long period seems to be an important factor for the transition from disorder state to equilibrium state, despite the possible variation in flux and in composition of the hydrothermal fluids.

ACKNOWLEDGEMENTS

This research was partially supported by the Graduate Fellowship of the Daewoo Foundation granted to the first author.

REFERENCES

Arnason, J. G. and Bird, D. K. (1992) Formation of zoned epidote in hydrothermal systems. In *Water-Rock Interaction*, Y. K. Kharaka and A. S. Maest, Eds., 1473-1476.

Bancroft, G. M., Maddock, A. G., and Burns, R. G. (1967) Applications of the Mössbauer effect to silicate mineralogy-1: Iron silicates of known crystal structure. Geochim. Cosmochim. Acta, 31, 2219-2246.

Bird, D. K. and Helgeson, H. C. (1980) Chemical interaction of aqueous solutions with epidote -feldspar mineral assemblages in geologic systems. I. Thermodynamic analysis of phase relations in the system CaO-FeO-Fe_2O_3-Al_2O_3-

SiO_2-H_2O-CO_2. Am. Jour. Sci., 280, 907-941.

Bird, D. K. and Helgeson, H. C. (1981) Chemical interaction of aqueous solutions with epidote -feldspar mineral assemblages in geologic systems. II. Equilibrium constraints in metamorphic/geothermal processes. Am. Jour. Sci., 281, 576-614.

Bird, D. K., Schiffman, P., Elders, W. A., Williams, A. E., and McDowell, S. D. (1984) Calc-silicate mineralization in active geothermal systems. Econ. Geol., 79, 671-695.

Bird, D. K., Cho, M., Janik, C. J., Liou, J. G., and Caruso, L. J. (1988) Compositional, order/disorder, and stable isotope characteristics of Al -Fe epidote, state 2-14 drill hole, Salton Sea geothermal system. Jour. Geophys. Res., 93-B11, 13, 135-13, 144.

Caruso, L. J., Bird, D. K., Cho, M., and Liou, J. G. (1988) Epidote-bearing veins in the state 2-14 drill hole: Implications for hydrothermal fluid composition. Jour. Geophys. Res., 93-B11, 13,123-13,133.

Deer, W. A., Howie, R. A., and Zussman, J. (1986) Rock-Forming Minerals. vol. 1B : Disilicates and Ring Silicates, 2nd Ed., 2-134.

Dollase, W. A. (1973) Mössbauer spectra and iron distribution in the epidote group minerals. Zeitschrift für Kristallographie, 138, 41-63.

Farmer, V. C. (1974) The layer silicates. In *The Infrared Spectra of Minerals*. V. C. Farmer, ed. London: Mineralogical Society, 331-363.

Franz, G. and Selverstone, J. (1992) An empirical phase diagram for the clinozoisite-zoisite transformation in the system $Ca_2Al_3Si_3O_{12}(OH)$- $Ca_2Al_2Fe^{3+}Si_3O_{12}(OH)$. Am. Mineral., 77, 631-642.

Fripiat, J. J. (1982) Application of far infrred spectroscopy to the study of clay minerals and zeolites. In *Developments in Sedimentology*. v. 34: Advanced techniques for clay mineral analysis, J. J. Fripiat, ed. Elsevier, Amsterdam. 191-210.

Grapes, R. and Watanabe, T. (1984) Al-Fe^{3+} and Ca-Sr^{2+} epidotes in metagreywacke-quartzofeldspathic schist, Southern Alps, New Zealand. Am. Mineral., 69, 490-498.

Ishii, M., Shimanouchi, T., and Nakahira, M. (1967) Far infrared absorption spectra of layer silicates. Inor. Chim. Acta, 1, 387-392.

Keith, T. E. C., Muffler, L. J. P., and Cremer, M. (1968) Hydrothermal epidote formed in the Salton Sea geothermal system, California. Am. Mineral., 53, 1635-1644.

Kim, S. J., Choo, C. O., Park, H. I., and Noh, J. H. (1991) Mineralogy and genesis of hydrothermal deposits from the southeastern part of Korean peninsula: (2) Bobae sericitic deposit. Jour. Mineral. Soc. Korea, 4, 93-114.

Kim, S. J., Choo, C. O., and Kim, W. S. (1994) Mineralogy and genesis of hydrothermal deposits in the southeastern part of Korean peninsula: (5) Deogbong deposit. Jour. Mineral. Soc. Korea, 7, 25-39.

Langer, K. and Raith, M. (1974) Infrared spectra of Al-Fe(III)- epidotes and zoisites, $Ca_2(Al_{1-p}Fe^{3+}_p)Al_2O(OH)[Si_2O_7][SiO_4]$. Am. Mineral., 59, 1249-1258.

Langer, K. and Lattard, D. (1980) Identification of a low-energy OH-valence vibration in zoisite. Am. Mineral., 65, 779-783.

Laperche, V. and Prost, R. (1991) Assignment of the far-infrared absorption bands of K in micas. Clays and Clay Mineral., 39, 281-289.

Maddock. A. G. (1985) Mössbauer spectroscopy in mineral chemistry. In *Chemical Bonding and Spectroscopy in Mineral Chemistry*. J. Berry, and J. Vaughan, Eds., 141-208. Champman and Hall.

Moon, J. W. (1994) Genetic environment and mineralogy of the Bobae deposit. 120p. M.S. thesis, Yonsei university.

Myer, G. H. (1965) X-ray determinative curve for epi-dote. Am. Jour. Sci.. 263, 78-86.

Paesano, A., Kunrath, J. I., and Vasquez, A. (1983) A ^{57}Fe Mössbauer study of epidote. Hyperfine Interactions, 15-16, 841-844.

Patrier, P., Beaufort, D., and Meunier, A. (1991) Determination of the nonequilibrium ordering state in epidote from the ancient geothermal field of Saint Martin: Application of Mö ssbauer spectroscopy. Am. Mineral., 76, 602-610.

Prost, R. and Laperche, V. (1990) Far-infrared study of potassium micas. Clays and Clay Mineral., 38, 351-355.

Raith, M. (1976) The Al-Fe(III) epidote miscibility gap in a metamorphic profile through the penninic series of the Tauern window, Austria. Contrib. Mineral. Petrol., 57, 99-117.

Redhammer, G. J., Beran, A., Dm achs, E., and Amthauer, G. (1993) A Mössbauer and X-ray diffraction study of annites synthesized at different oxygen fugacities and crystal chemical implications. Phys. Chem. Mineral., 20, 382-394.

Schroeder, P. A. (1990) Far infrared, X-ray powder diffraction, and chemical investigation of potassium micas. Am. Mineral., 75, 983-991.

Seki, Y. (1959) Relation between chemical composition and lattice constants of epidote. Am. Mineral., 44, 720-730.

Shikazono, N. (1984) Compositional variations in epidote from geothermal areas. Geochem. Jour., 18, 181-187.

Vedder, W. (1964) Correlations between infrared spectrum and chemical composition of mica. Am. Mineral., 49, 736-768.